ePublishing

ΕΘΝΙΚΟ ΚΕΝΤΡΟ ΤΕΚΜΗΡΙΩΣΗΣ
EKT NATIONAL DOCUMENTATION CENTRE

HNPS Advances in Nuclear Physics

Vol 16 (2008)

HNPS2008

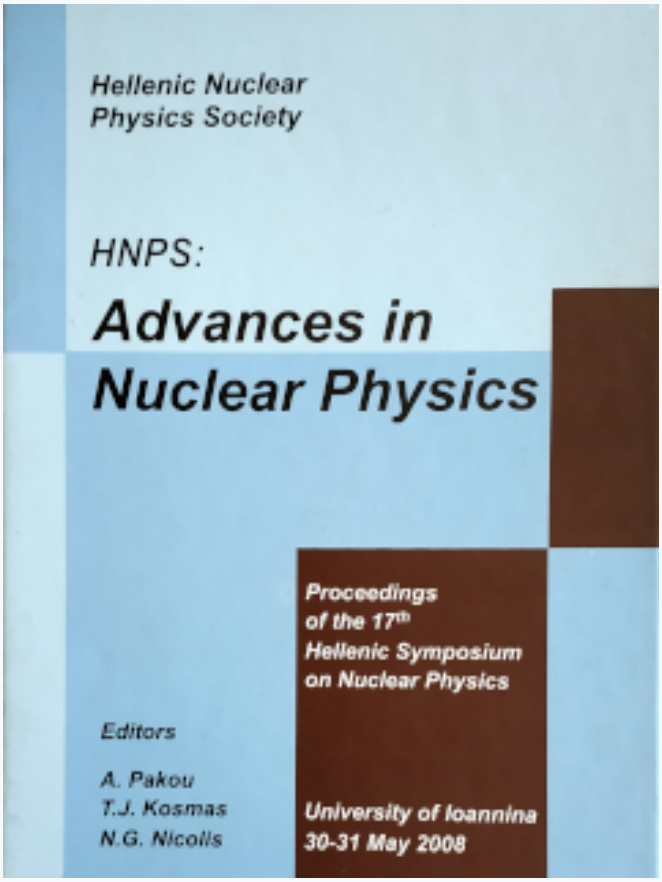

Development of a portable micro-XRF spectrometer and its application for the characterization of ancient and historical metal alloys

V. Kantarelou, D. Sokaras, Ch. Zarkadas, A.-G. Karydas

doi: 10.12681/hnps.2600

To cite this article:

Kantarelou, V., Sokaras, D., Zarkadas, C., & Karydas, A.-G. (2020). Development of a portable micro-XRF spectrometer and its application for the characterization of ancient and historical metal alloys. *HNPS Advances in Nuclear Physics*, *16*, 221–229. https://doi.org/10.12681/hnps.2600

https://epublishing.ekt.gr | **e-Publisher:** EKT | **Downloaded at:** 09/05/2026 21:13:56

Development of a portable micro-XRF spectrometer and its application for the characterization of ancient and historical metal alloys

V. Kantarelou, D. Sokaras, Ch. Zarkadas and A. G. Karydas

Institute of Nuclear Physics, NCSR Demokritos, 15310, Athens, Greece

Abstract

A portable micro-XRF spectrometer utilizing X-ray optics (polycapillary X-ray lens) has been developed and applied for the characterization of the surface of ancient and historical metal alloys within the Mediterranean basin. The spectrometer has been fully characterized with respect to its spatial resolution, elemental excitation efficiency and sensitivity. A dedicated quantification algorithm was also developed, whereas new analytical procedures were explored towards the optimum implementation of the technique in the field of conservation.

1 Introduction

The principle of X-ray Fluorescence (XRF) is the inner-shell ionization of atoms by an exciting X-ray beam and the subsequent emission of characteristic X-rays with energy specific for each element of the periodic table. The identification of the atoms that compose a material is possible with the use of energy dispersive detection system (qualitative analysis). During the last decade, the localization of the exciting X-ray beam was successfully addressed through the rapid development of high performance optical devices, such as polycapillary X-ray lenses, capable of efficient capturing, transmitting and focusing the X-ray beams down to a diameter of a few tens of micrometers ([1–5]). The latter improvement in the instrumentation lead to analysis of microscopic-surface details and added to the XRF technique, apart from the possibility to perform qualitative and quantitative elemental analysis, the important option for spatially resolved elemental information. Evidently, the micro-XRF spectroscopy enables even on the site, ie museum environment, to perform in a reasonable measuring time two dimensional scanning of the

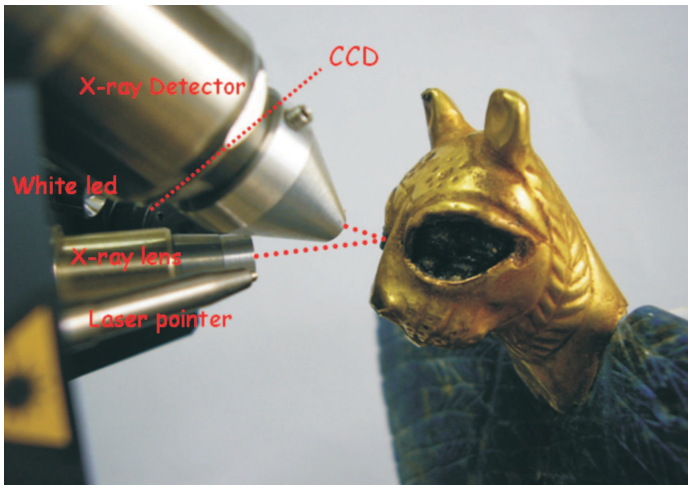

Fig. 1. Photo of the micro-XRF measuring probe. The artifact is a Headed Eagle with lapis lazuli and gold dated to 3000 B.C. Early Bronze Age, National Museum of Damascus. ©PROMET [6]

interested area deducing a detailed spatially resolved intensity (concentration) distribution of the detected elements. Improving the methodological and quantitative aspects of the micro-XRF analysis, useful information regarding the manufacture techniques, the composition of raw materials and associated trace elements may be revealed supporting the archaeometallurgical research and conservation of a collection.

2 Experimental

The Demokritos portable micro-XRF spectrometer has been developed within FP6 project PROMET (www.promet.org.gr, [6]) based on commercial, customized, state of the art hardware components in an experimental configuration to fulfil certain analytical requirements; high flux and very good spatial resolution for the exciting beam at the sample position ($\sim 40 - 100\ \mu m$), an X-ray detector that may proceed count rates up to $100kHz$ without significant dead time losses and deterioration of its energy resolution, potential to observe in detail and record the area analyzed. The spectrometer probe consists of an X-ray micro focus Rh-anode tube (spot size $50\mu m \times 50\mu m$, max $50kV$, max $0.6mA$, $30W$ maximum power consumption, Be window $0.2mm$ thickness), a polycapillary X-ray lens as a focusing optical element (IfG, focal f2 distance = $21.2mm$, gain factor that varies between 3625 - 4900 - 1200 for exciting energies in the intervals 3-5, 10-15 and 25-30 keV, respectively). The X-ray detection chain consists of an electro-thermally cooled $10mm^2$ silicon drift detector (X-Flash, 1000B) with FWHM equal to $146eV$ at $10kcps$ coupled with a digital signal processor. By increasing the count rate up to $100kHz$ only a 20% worsening of the FWHM is observed. A color CCD camera (13

times magnification) and a dimmable white LED for sample illumination a laser spot are important hardware utilities that support the reproducible positioning of the measuring probe, the visualization and recording of the area analysed. The various components of the spectrometer probe are presented in Figure 1 during the analysis of an artefact at the National Museum of Damascus. Three different stepping motors, coupled with the spectrometer head, allow its three-dimensional movement, setting precisely the analysis spot at the focal distance of the polycapillary lens, providing also the possibility of pc-controlled elemental mapping studies.

2.1 Characterization of the micro-XRF spectrometer

2.1.1 Spatial resolution

The spatial resolution of the micro-XRF was determined by scanning various metal wires (Ti, Fe, Cu/Sn, Mo and Ag) using $10\mu m$ step size. The diameters of the wires were selected to be 25 or $50\mu m$, less than the expected set-up resolution.
The intensity profiles were measured by employing unfiltered and filtered (with a Ni foil of $25\mu m$ as filter) excitation,and were found to exhibit as expected a Gaussian-like dependence. The spatial resolution was found to vary approximately between $100-40\mu m$ for unfiltered excitation and characteristic X-ray energies between $3-25keV$, respectively. Using a filtered exciting beam, a significant decrease ($\sim 25\%$) of the FWHM of the intensity profile was measured due to the fundamental property of the polycapillary lens to focus higher energies at smaller spot sizes and the opposite (it is noted that the filter absorbs preferentially the lower energies of the exciting spectrum and relatively enhances the more energetic one). The overall energy dependence of the spatial resolution versus energy follows the general trend that as the energy increases, the focal size is decreased. The slight increase observed above $20keV$ can be attributed to the halo effect produced by the primary tube X-rays that penetrate the complete capillary optic [3].

2.1.2 Elemental sensitivities

The elemental $K\alpha$ and $L\alpha$ production yields (elemental sensitivities) of the micro-XRF spectrometer were experimentally determined by means of a series of pure single element or compound thin targets with an area density of about $50\mu g/cm^2$. In Figure 2, the dependence of the $K\alpha$ and $L\alpha$ production yields expressed in (counts/s) per ($\mu g/cm^2$), are plotted versus the energy of the respective characteristic X-ray. The shape of the observed dependence is governed and modulated by the energy dependence of the tube excitation

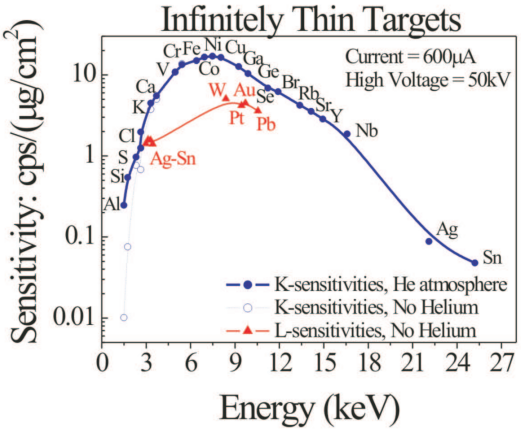

Fig. 2. Elemental excitation response of the micro-XRF spectrometer, as it is expressed in terms of the fluorescent intensity per unit mass of infinitely thin targets.

spectrum and by the lens transmission efficiency. It should be noted that for elements with low atomic number ($Z < 17$), the corresponding intensities decrease relative to the one produced by the transition metals ($20 < Z < 32$) by one or two orders of magnitude only when the measurements are performed in Helium atmosphere.

2.1.3 Minimum detection limits

The elemental sensitivity range of the micro-XRF spectrometer, namely the Minimum Detection Limit (MDL) was determined in terms of absolute mass (ng) (using a set of infinitely thin targets), or as bulk concentration ($\mu g/g$) (using a set of lead-free standard reference glassy materials). Referring to the elements that emit K- characteristic X-ray lines with energies between $4-17keV$ and to the following measuring conditions, $50kV$, $600\mu A$ and $1000s$, the MDLs were found to be $1-2ng$, or between $5-10ppm$, respectively, comparable with published data [7,9].

2.2 Determination of the transmission efficiency of the lens and quantification procedure

In mirco-XRF analysis, a polycapillary X-ray lens is usually utilized in the excitation channel to collect efficiently, propagate and focus to a few tens of micrometers the exciting X-ray beam radiation. A polycapillary X-ray lens is a capillary bundle with hundreds or thousands of tiny hollow curved or taped glass tubes with diameters at the order of few microns. X-rays striking the interior of the glass tubes at grazing incidence are guided by total external

reflection. A variety of geometrical parameters selected during the manufacture process (the distances between the optic input/output and the source or the focusing point respectively, the lens length, etc.), define the analytical performance (transmission efficiency, spatial resolution, gain) of the lens for each specific energy interval. The X-ray lens introduces major difficulties in quantification, since its transmission efficiency being highly dependent on the transmitted X-ray energy results to a significant and not easily predicted modification of the energy distribution of the primary tube spectrum A theoretical fundamental parameter approach (FPA) model was developed based on an analytical description for the tube emission spectrum [10] and on a transmission efficiency expressed as polynomial of 5th degree versus energy. (The transmission efficiency is defined as the intensity of the transmitted X-rays relative to the corresponding one entering into the lens.) Measured and theoretically predicted characteristic K- or L- line intensities emitted by a large set of pure single element or compound targets, with infinite or very small thickness were compared through a χ^2 minimization procedure using fitted parameters the coefficients of the transmission efficiency function. The agreement between theoretical and experimental elemental intensities at the convergence minimum was equal or better than 10%. The developed FPA model was next validated in reproducing concentrations of ten NIST and BAM standard reference glasses with deviations less than $10\% - 15\%$.

3 Results and discussion

3.1 Identification of corrosion products

The surface of the copper coupon CNR128 (typical bulk composition Cu: 91.3%, Sn: 7.5%, Pb: 0.2%), artificially and naturally corroded by the CNR-ISMN group, was examined across a line by means of a micro-XRF scanning (Figures 3(a) and 3(b)). The line scan parameters were: tube voltage $50kV$, tube current $600\mu A$, scanned area=$5mm^2$, step size= $0.1mm$, measurement time/step=$30s$. Figure 3(c) shows the variation of the $Cu - K\alpha$ and $Cl - K\alpha$ X-ray intensities deduced by the accumulated spectra. Two distinct regions were identified, one with high copper and another with increased copper and chlorine. Tin showed a modest variation without extreme values; however at spot #9 receives its relatively maximum value (where copper had its lowest intensity and chlorine was not detected at all). The observed variation of the $Cu - K\alpha$ and $Cl - K\alpha$ characteristic X-ray intensities is in accordance with the colors observed. In the pale green area, Cu and Cl coexist, whereas in the green area there is Cu and minor amounts of Sn suggesting the presence of paratacamite in the former case and malachite in the latter. Figure 3(d) shows the corresponding micro-XRF spectra from the two areas.

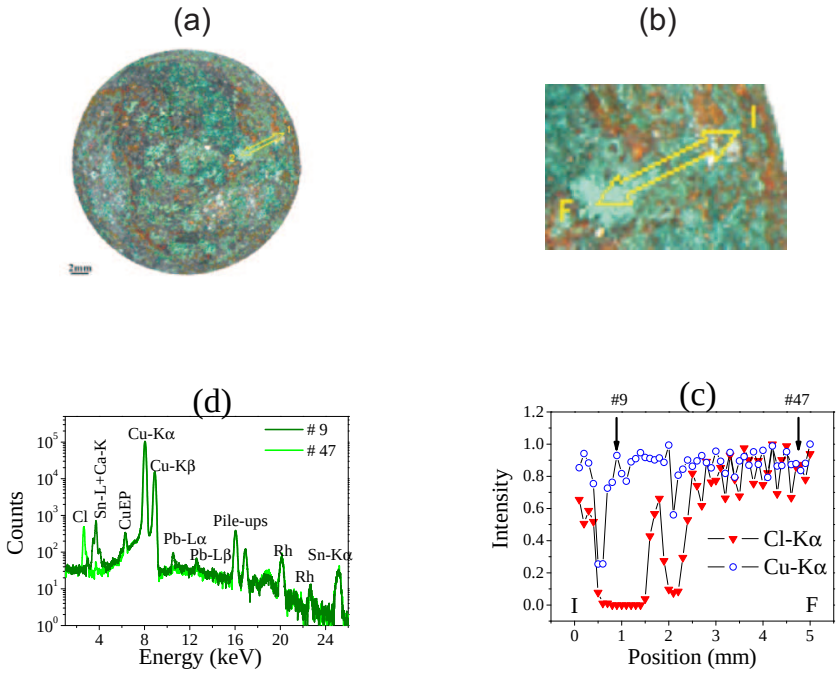

Fig. 3. Micro-XRF analysis of a copper coupon (CNR128), with typical composition Cu: 91.3%, Sn: 7.5%, Pb: 0.2%. The line scan parameters were: tube voltage $50kV$, tube current $600\mu A$, length of the scanned area=$5mm^2$, step size=$0.1mm$, measurement $time/step = 30s$. In Figs. (a) and (b) the scanned area is shown including areas mainly with green or light-pale green color. (c) The variation of the $Cu - K\alpha$ and $Cl - K\alpha$ characteristic X-ray intensities is in association with the colors observed, namely, Cu and Cl coexist in the light-pale green area, whereas in the green one Cu and Sn, respectively. In Fig. (d), corresponding micro-XRF spectra from the two areas are presented that suggest the presence of paratacamite (#47) and of malachite together with minor amounts of cassiterite (#9).

3.2 Gilding technology of 16th century armoury

The Armoury Palace in Malta was surveyed to get a broad overview of the nature of the materials constituting the collection. Gilding remains could still be observed on several arms (Armours $\#6, \#9, \#12, \#14 - 17$, [11]). Results of the gilding analyses suggest that most of the artifacts were fire-gilded. In the latter technique, the gilding layer is procured as a gold-mercury amalgam which is applied onto a surface that is first pre-treated with copper acetate (Cu promotes Au bonding to Fe). The mercury is then removed by heating [12]. In Figures 4(a)-(b) the investigated area on armour #6 is shown. The area mapping was performed at $50kV$, 600μ, $100\mu m$ step size and $20s/step$, as measuring conditions. The area mapping for Hg and Au intensities shows similar pattern (Figures 4(c)-(d)), whereas the corresponding one for Cu (Figure 4(e)) presents differences. The mean intensities of Hg / Au versus Au, from area mappings on three different armours are presented in Figure 5. The

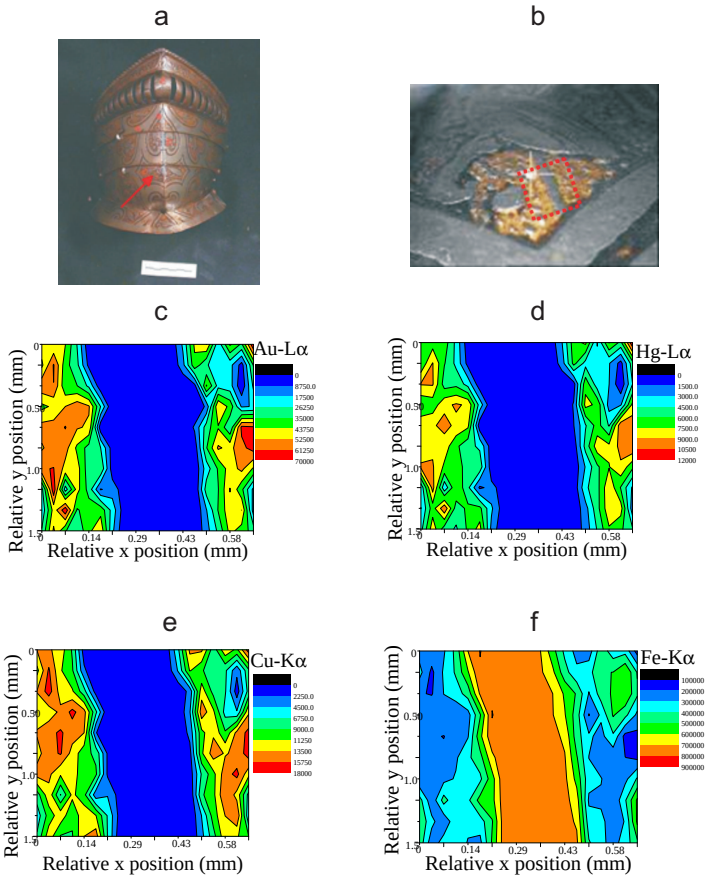

Fig. 4. Gilding areas of artefact Arm 6 analysed with the milli- and micro-XRF spectrometers: (a), (b): Photos of the armour and the scanned area, respectively. (c)-(f): Results of the micro-XRF area mapping. The intensity variation of $Au-L\alpha$ and $Hg-L\alpha$ characteristic X-rays is identical, whereas the $Cu-K\alpha$ one shows some intensity variations, although it resembled the general trend followed by Au and Hg lines. Operating conditions: $50kV$, 600μ, "unfiltered excitation", $20s/step$, $0.1mm/step$.

mean values where deduced among a subgroup of the area map spots, where the Au intensity varies between $0-10\%$, $10-20\%$, $30-40\%$ etc with respect to its maximum value. It can be observed, that the intensity ratio of Hg/Au is almost constant for each of the armours, but presenting a very close value among them. This result confirms a perfect bonding of Hg and Au in the amalgam. In addition, it may also indicate similarities in the applied gilding technique among different armours.

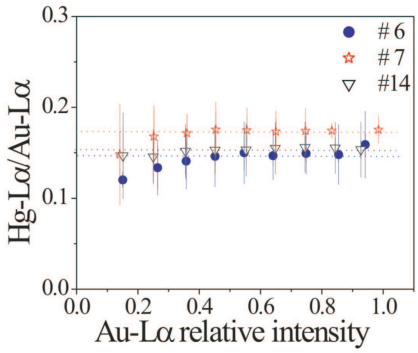

Fig. 5. Mean intensities of Hg/Au versus Au, from area mappings on three different armours (#6, 7 and #14) The mean values where deduced among a subgroup of the area map spots, where the Au intensity varies between 0-10%, 10-20%, 30-40% etc with respect to its maximum value.

4 Conclusions

Within the PROMET project, a mobile micro-XRF spectrometer, based on an industrial prototype, but with customized hardware components, has been characterized and applied in surveying museum metals collections. A systematic study of the micro-XRF spectrometer characteristics was undertaken regarding the analytical description of its elemental excitation response, spatial resolution and analytical sensitivity. The experience of applying the non-invasive micro-XRF analysis in-situ was found useful and promising. At first, an assessment of the state of preservation of an artefact can be performed by defining the gamut of corrosion products present on its surface and identifying surface finishing technique. Needless to say, the analytical information could be supported and integrated by other non-invasive techniques; however, the role of the in-situ micro-XRF analysis seems to be unique as a first elemental screening analysis that provides insight into the manufacture and the preservation state of archaeological and historical metal alloys.

5 Acknowledgments

The present work was supported by the FP6 European project, PROMET (FP6-2002-INCO-MPC1). Also we acknowledge G.M. Ingo (CNR-ISMN, Italy) for preparing the corroded copper coupon and Dr. C. Degrigny, Dr S. Golfomitsou (Heritage Malta) for organizing and supporting the in-situ measurements at Armoury Palace in Malta.

References

[1] Gormley, J. Jach, T. Steel, E. Xiao, Q.-F., X-Ray Spectrometry, 28(2):115-120,1999.

[2] Xie, J. Yan, Y. Ding, X. He, Y. Pan, Q. X-Ray Spectrometry, 29(4):305-309, 2000.

[3] Haschke, H. Haller, M. X-Ray Spectrometry, 32(3):239-247,2003.

[4] Bjeoumikhov, A. Langhoff, N. Wedell, R. Beloglazov, V. Lebedev, N. Skibina, N. X-Ray Spectrometry, 32(3):172-178,2003.

[5] Bjeoumikhov, A. Langhoff, N. Bjeoumikhova, S. Wedell, R. Review of Scientific Instruments, 76(6):1-7,2005.

[6] A.G.Karydas, D.Anglos and M.A. Harith, Mobile Micro-XRF and LIBS Spectrometers for Diagnostic Micro-Analysis of Ancient Metal Objects. In Metals and Museums in the Mediterranean: Protecting, Preserving and Interpreting, ed. V.Argyropoulos, 2008

[7] Vittiglio, G. Bichlmeier, S. Klinger, P. Heckel, J. Fuzhong, W. Vincze, L. Janssens, K. Engstrom, P. Rindby, A. Dietrich, K. Jembrih-Simburger, D. Schreiner, M. Denis, D. Lakdar, A. Lamotte, A. 2004, Nuclear Instruments and Methods in Physics Research Section B, 213:693-698.

[8] Schreiner, M. Denis, D. Lakdar, A. Lamotte, A. Nuclear Instruments and Methods in Physics Research Section B, 213:693-698,2004.

[9] Cheng, L. Ding, X. Liu, Z. Pan, Q. Chu, X. Spectrochimica. Acta Part B, 62(8):817-823, 2007.

[10] H. Ebel, X-Ray Spectrometry. 28, (1999) 255-266.

[11] C.Degrigny, A.G. Karydas, S. Golfomitsou, V. Kantarelou, Ch. Zarkadas, D. Vella, METAL-07, Vol. 2, Innovative investigation of metal artifacts, pp. 26-34. 2007

[12] William A.R., 1977, Gold Bulletin, 10, pp115-117.